The spectral response of the SCUBA-2 850 and 450 micron photometric bands

David A. Naylor*[a], Brad G. Gom[a], Sherif AbdElazim[a], Per Friberg[b], Daniel Bintley[b], Wayne S. Holland[c], Michael J. MacIntosh[c], Peter A. R. Ade[d], Carole E. Tucker[d]
[a]Institute for Space Imaging Science, University of Lethbridge, Alberta, T1K 3M4, Canada; [b]Joint Astronomy Centre, 660 N. A'ohoku Place, University Park, Hilo, Hawaii, 96720, USA; [c]UK Astronomy Technology Centre, Royal Observatory, Edinburgh, Blackford Hill, Edinburgh, EH9 3HJ, UK; [d]Cardiff School of Physics and Astronomy, Cardiff University, Cardiff, CF24 3AA,UK

ABSTRACT

SCUBA-2 is a wide-field submillimeter bolometer camera operating at the James Clerk Maxwell Telescope. The camera has twin focal planes, each with 5120 superconducting Transition Edge Sensors, which provide simultaneous images in two filter bands at 450 and 850 microns matched to the atmospheric windows. Detailed knowledge of the optical filter profiles that define these bands is important for estimating potential contamination from the prevalent CO J = 3-2 and CO 6-5 line emission, and correctly interpreting the effects of the source spectral index on photometric observations. We present measurements of the spectral response of SCUBA-2 obtained with FTS-2, the ancillary Fourier transform spectrometer instrument at the JCMT. The spectral measurements will be compared with the predicted filter profile determined from the linear combination of the individual filter profiles present in the SCUBA-2 optical train.

Keywords: SCUBA-2, spectral, filter, profiles, Fourier Transform Spectrometer

1. INTRODUCTION

SCUBA-2 is a wide-field submillimeter bolometer camera operating at the James Clerk Maxwell Telescope[1]. The camera has twin focal planes, each with 5120 superconducting Transition Edge Sensors, which provide simultaneous images in two spectral bands centred at 450 and 850 μm. Several optical filters, operating at different temperatures, are used to define these spectral bands, which are matched to the atmospheric windows shown in Figure 1. The transmissions of the cryostat window and the individual filters, including the dichroic, that make up the optical train have been measured in the laboratory at room temperature[2]. Their integrated performance at cryogenic temperatures, however, including any fringing due to reflections between filters in the cryostat, cannot be easily modeled. A detailed knowledge of the spectral bandpass of SCUBA-2 is important for estimating potential contamination from the prevalent CO J = 3-2 and CO 6-5 line emission, and correctly interpreting the effects of the source spectral index on photometric observations. We present measurements of the spectral response of SCUBA-2 obtained with FTS-2, the ancillary Fourier transform spectrometer (FTS) instrument[3,9] at the JCMT.

Designed to fill a niche between the high spectral resolution, but low pixel count JCMT facility instrument HARP-B[4] and the wider band but lower spectral and spatial resolution SPIRE FTS on the Herschel space observatory[5,6], FTS-2 provides moderate resolving powers of R ~ 10 to 5000 across the 450 and 850 μm atmospheric transmission windows over an instantaneous field of view of ~5 arcmin[2]. FTS-2 measures the difference between radiation entering the two input ports of the interferometer. By placing an ambient blackbody in one port and a heated blackbody in the second port, the resulting interferograms can be processed to provide, simultaneously, the spectral response of all pixels in the 450 and 850 μm sub-arrays that are utilized by FTS-2. These measurements can then be compared with the predicted system spectral response determined from the linear combination of the individual filter profiles present in the SCUBA-2 optical train, which have been measured in the laboratory.

A schematic of the various filters that are employed in SCUBA-2 is shown in Figure 2. The temperature, optical bandwidth and transmission of the components are listed in Tables 1 and 2. The spectral transmission of each component, as measured at room temperature in the laboratory, is shown in Figure 3.

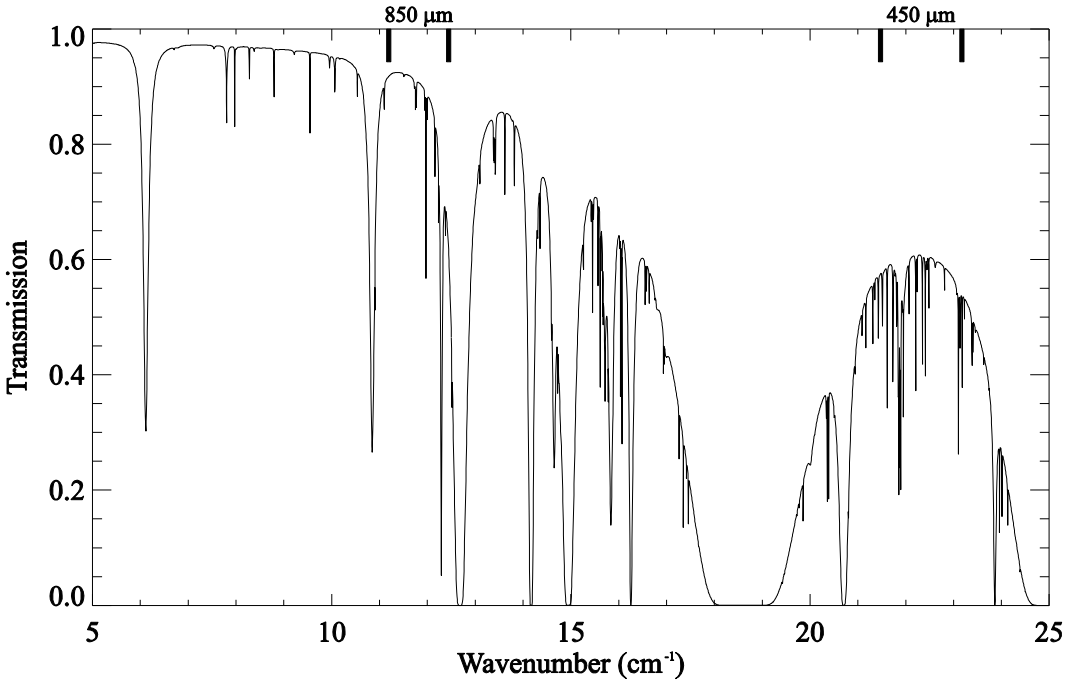

Figure 1: The theoretical atmospheric transmission above Mauna Kea for 0.5 mm precipitable water vapor, calculated using the BTRAM radiative transfer model[7]. The thick bars represent the approximate FWHM of the 850 and 450 µm SCUBA-2 filter bands.

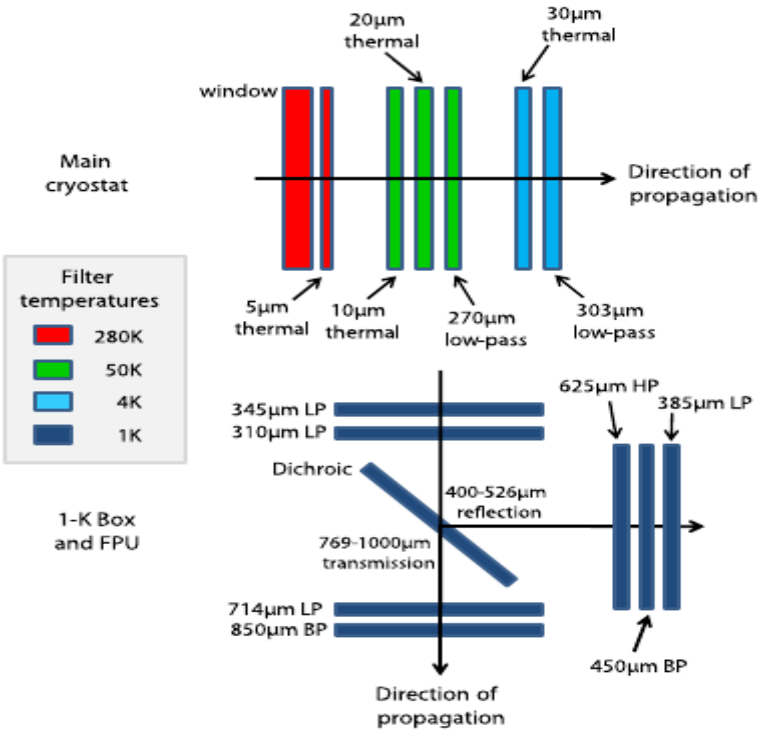

Figure 2. Schematic of the filters installed in SCUBA-2 and their operating temperature; BP, LP and HP represent band-pass, low-pass and high-pass, respectively[1].

Table 1. Specifications of the SCUBA-2 filters.

Filter Location	Filter name	Temperature (*K*)	Pass band (cm^{-1})	Transmission (%)
Window	450	300	21.1-23.5	>90
	850	300	11-12.3	>90
Inside 300K window	C_B0	300	5-30	>95
Radiation shield outer	C_B1	60	5-30	>95
Rad. shield middle	C_B2b	60	5-30	>95
Radiation shield inner	C_B2a	60	5-30	>95
Helium shield	C_B3a	4	5-30	>95
Helium shield	C_B3b	4	5-40	>90
Cold stop (outer)	C_B4a	1	5-40	>90
Cold stop (inner)	C_B4b	1	5-40	>90
Array edges	450_B5	0.1	20-optical	>90
	850_B5	0.1	10-16	>90
Array Bandpass	450_BP	0.1	21.1-23.5	>70
	850_BP	0.1	11-12.3	>70

Table 2. Specification of the SCUBA-2 dichroic.

Temperature (K)	Reflection		Transmission	
	Frequency Range (cm^{-1})	Transmission (%)	Frequency Range (cm^{-1})	Transmission (%)
1	19-25	>90	10-13	>90

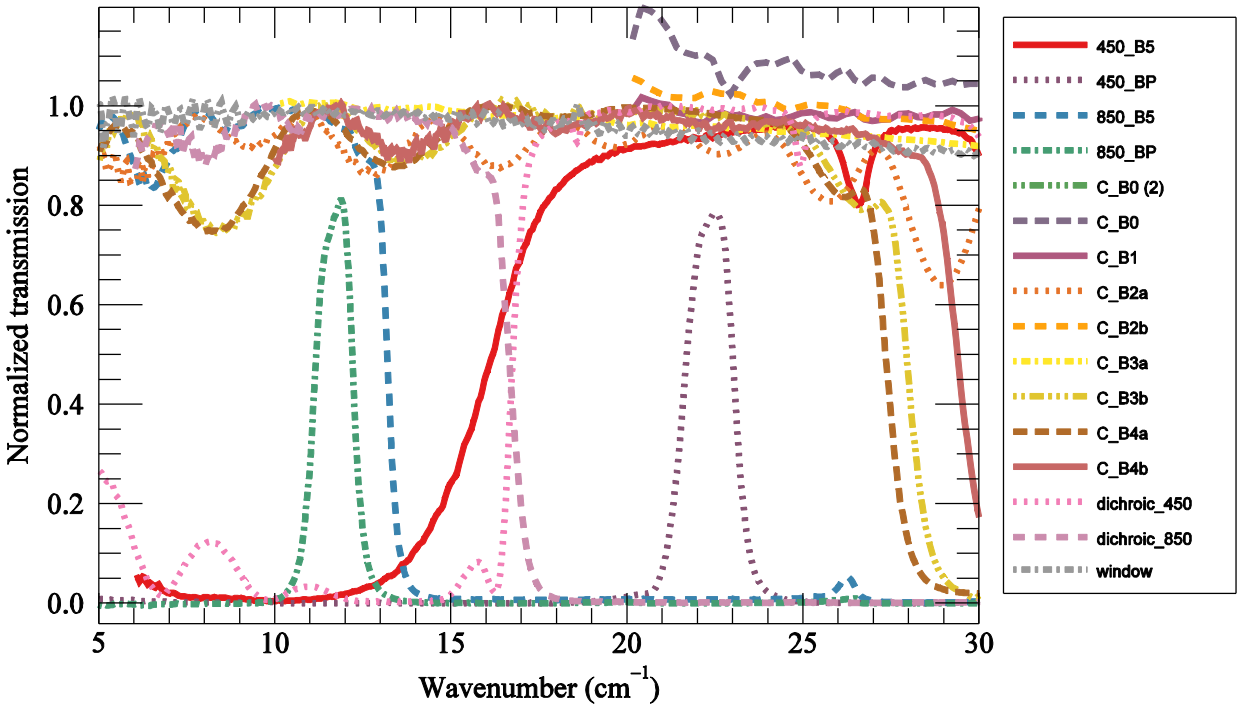

Figure 3. The spectral profiles of the optical components within SCUBA-2, measured individually in the laboratory at room temperature[2].

2. DETERMINING THE SPECTRAL RESPONSE OF SCUBA-2

Since the signal produced in each complementary FTS-2 output port represents the interferometric difference of the two input ports, blackbodies of different known temperatures must be placed in the two input ports in order to determine the spectral response of SCUBA-2, $F(\sigma)$, as an integrated system. The spectrum measured by FTS-2, $O(\sigma)$, can be expressed as the difference between two blackbodies of emissivity ε_A, ε_B, and temperature T_A, T_B, respectively, illuminating a bolometer having an area solid angle product of $A\Omega$, with an overall system efficiency, assumed to be independent of wavelength, η, as:

$$O(\sigma) = F(\sigma)\eta\left[\varepsilon_A B(\sigma, \mathrm{T_A}) - \varepsilon_B B(\sigma, T_B)\right] A\Omega \tag{1}$$

where the spectral radiance is given by the Planck function, $B(\sigma, T)$:

$$B(\sigma, T) = 2hc^2\sigma^5 \frac{1}{e^{\frac{hc\sigma}{kT}} - 1} \qquad \text{W sr}^{-1}\ \text{m}^{-2}\ (\text{cm}^{-1})^{-1} \tag{2}$$

where h is the Planck constant, c the speed of light, k the Boltzmann constant, σ the wavenumber and T the temperature. To account for the slightly different coupling efficiencies of the two ports of FTS-2, the spectral response of SCUBA-2 is determined from a second differential measurement in which the temperature of one of the blackbody sources is varied while the other held constant. In this case the two measurements can be expressed as:

$$O_1(\sigma) = F(\sigma)\eta\left[\varepsilon_A B(\sigma, T_{A1}) - \varepsilon_B B(\sigma, T_B)\right] A\Omega \qquad \text{W } (\text{cm}^{-1})^{-1} \tag{3}$$

$$O_2(\sigma) = F(\sigma)\eta\left[\varepsilon_A B(\sigma, T_{A2}) - \varepsilon_B B(\sigma, T_B)\right] A\Omega \qquad \text{W } (\text{cm}^{-1})^{-1} \tag{4}$$

where T_{A1} and T_{A2} are the two temperatures of the heated blackbody. The difference between these two measurements becomes:

$$O_2(\sigma) - O_1(\sigma) = F(\sigma)\eta\,\varepsilon_A\left[B(\sigma, T_{A2}) - B(\sigma, T_{A1})\right] A\Omega \qquad \text{W } (\text{cm}^{-1})^{-1} \tag{5}$$

Finally, dividing by the difference between the Planck function corresponding to the two temperatures, and normalizing for the efficiency, emissivity and throughput terms (all assumed to be independent of wavelength), yields the instrumental relative spectral response function, $SRF(\sigma)$:

$$SRF(\sigma) = \frac{\left[O_2(\sigma) - O_1(\sigma)\right]}{\left[B(\sigma, T_2) - B(\sigma, T_1)\right]} \tag{6}$$

3. MEASUREMENTS

Two calibration sources consisting of sheets of Eccosorb[8], which has high emissivity at these wavelengths and thus a good approximation to a blackbody, were placed in the two input beams of FTS-2. One of the sources was mounted to a thin film heating element with adjustable temperature. The blackbody in Port 1 was held at constant temperature while that in Port 2 was operated at three temperatures with an uncertainty of ± 0.5 °C as listed in Table 3.

Table 3. Average temperatures of the blackbodies placed in the two FTS input ports during the spectral response function tests.

Port 2 Temperature	Port 1 Temperature
16.8 °C	7.7 °C
25.3 °C	8.1 °C
34.0 °C	8.4 °C

Ten high resolution (corresponding to $\Delta\sigma \sim 0.006$ cm^{-1}) interferograms were recorded for each of the three temperature settings listed in Table 3. Figure 4 shows the typical signal obtained near the zero path difference region of the

interferogram for a well behaved bolometer. The high signal-to-noise ratio and symmetry are evident. As discussed in a companion paper, the bolometers are susceptible to non-linearity arising from flux jumps within the detector readout electronic chain[9]. Upon Fourier transformation, the spectra were screened for non-linear effects, which are easy to diagnose in the spectral domain by studying the residual power in the harmonic regions of the spectrum[10], before co-addition. Figure 5 shows the resulting mean spectrum for pixel (19, 22) in the 850 μm band sub-array, s8c, when observing the blackbody at 34 and 16.8 °C in port 2, with port 1 viewing an ambient blackbody at 8.4 and 7.7 °C, respectively. The radiance curves derived from the Planck function for these temperatures is shown in Figure 6.

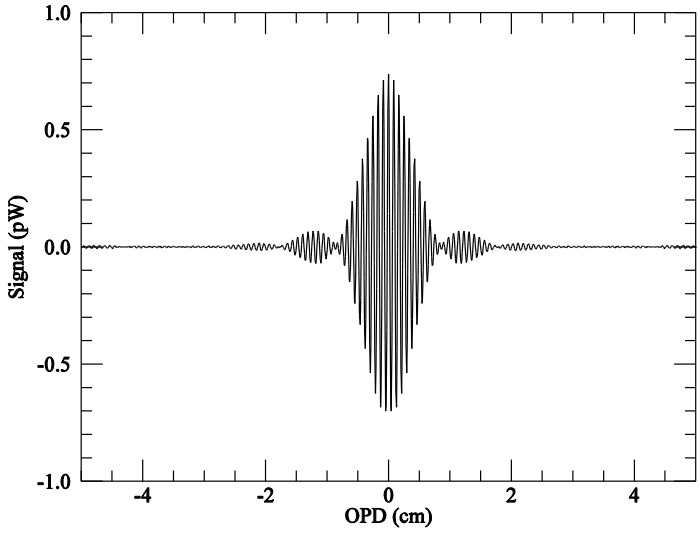

Figure 4: A representative interferogram pixel (19, 17) of the s8c subarray near the ZPD region. The symmetry and high signal-to-noise ratio are evident.

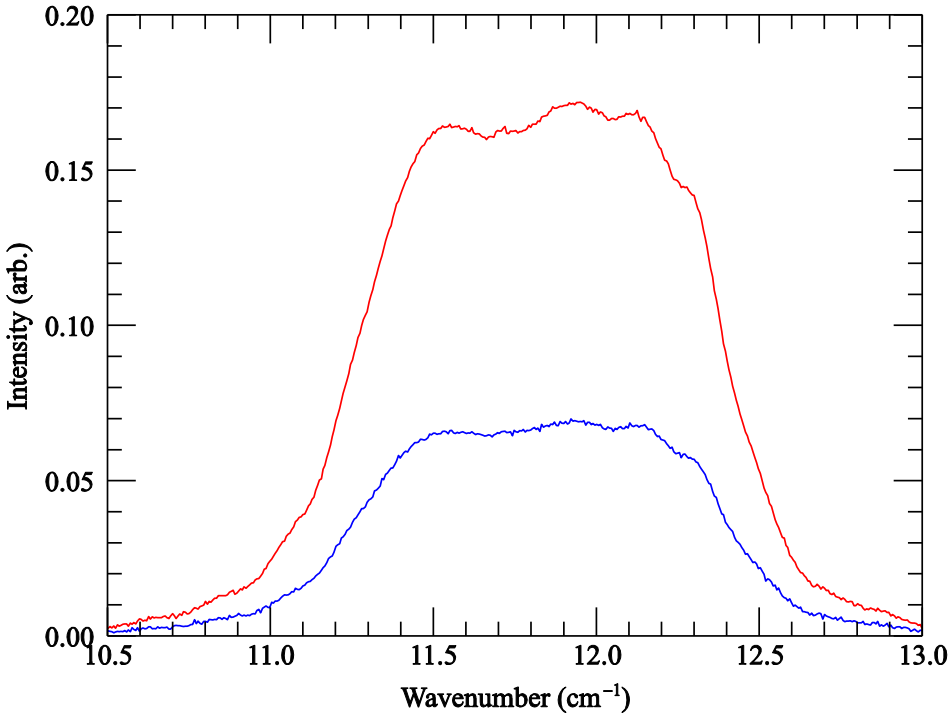

Figure 5: The mean spectrum for pixel (19, 22) in the 850 μm band sub-array (s8c) corresponding to heated blackbody temperatures of 34.0 °C (top) and 16.8 °C (bottom) in port 2, respectively. The reference blackbody temperatures in port 1 were 8.4 and 7.7 °C, respectively. The standard deviation across the spectral band is ~0.0013.

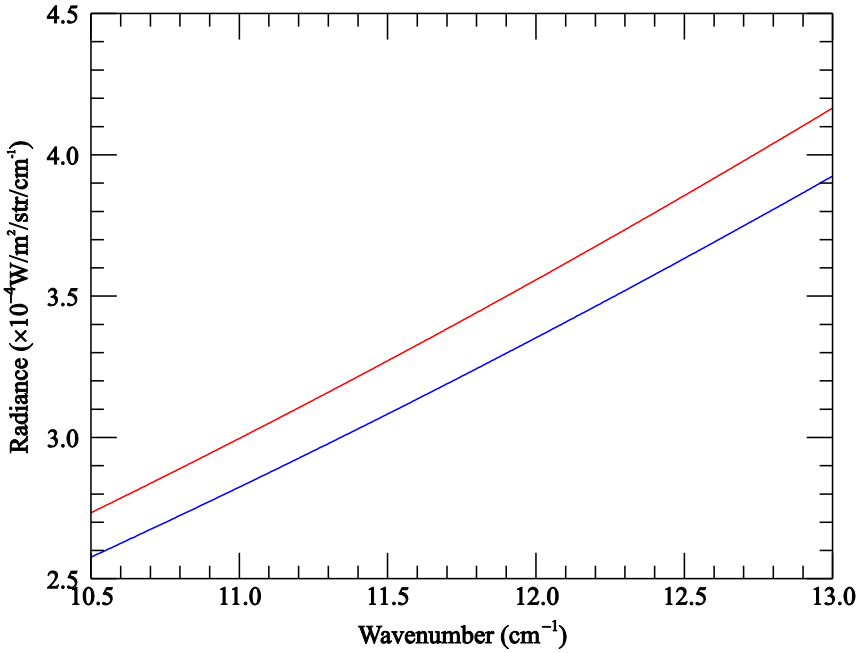

Figure 6: Theoretical Planck blackbody spectra in the 850 μm band for temperatures corresponding to the measurements in Figure 5. These temperatures and frequencies are in the Rayleigh-Jeans regime, therefore the spectra show a σ^2 dependence on frequency and linear dependence on temperature.

4. RESULTS

4.1 Measured SRF

The differences between the spectra shown in figures 5 and 6 are divided to yield the spectral response function (SRF) defined in equation 6. The SRF for a single bolometer is shown in Figure 7 and the mean SRF for all pixels that pass the non-linear screening threshold is shown in Figure 8.

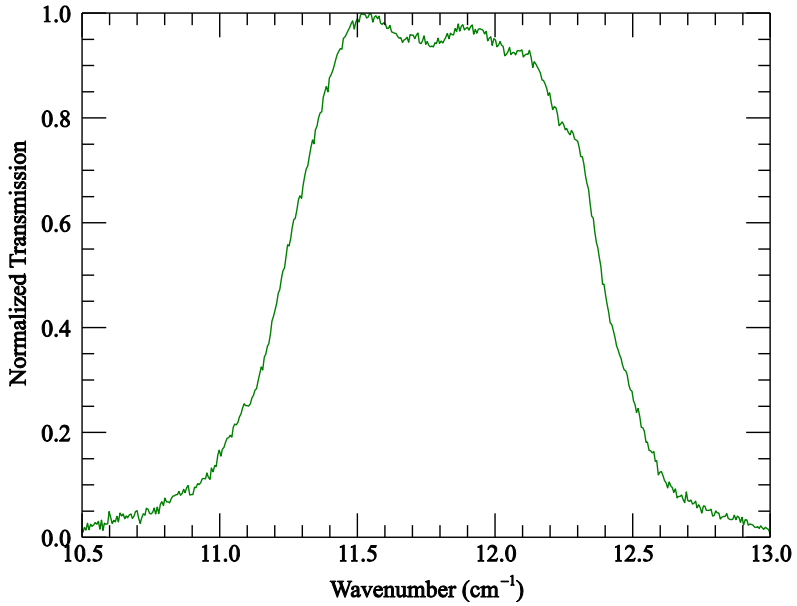

Figure 7: The spectral response function of bolometer (19, 22) in the 850 μm sub-array, s8c.

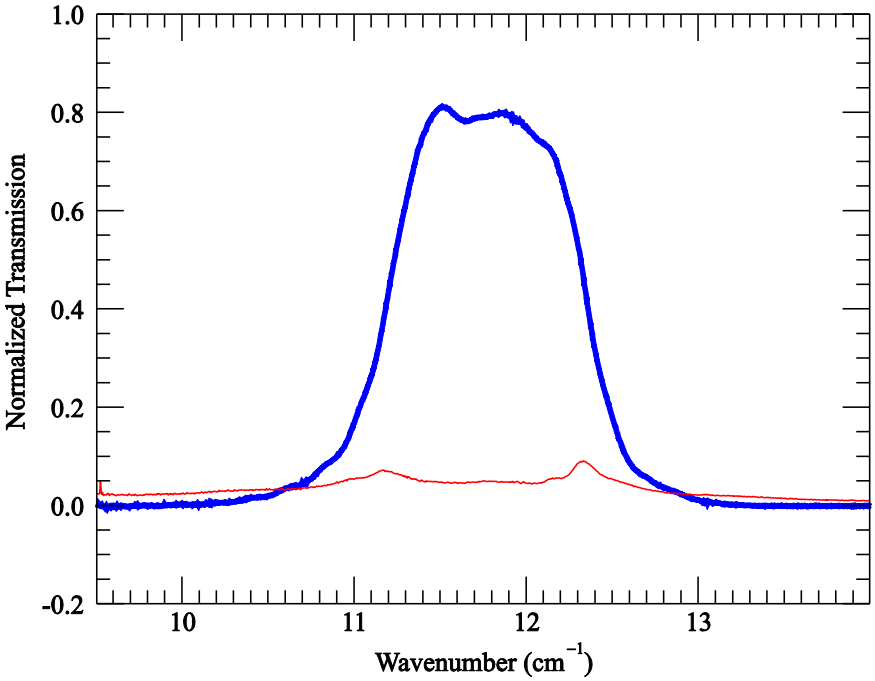

Figure 8: The normalized mean (blue) and standard deviation (red) of the spectral response function for all bolometers in the 850 μm band sub-array s8c. There are slight variations in the SRF edges and fringing for pixels across the FOV, as indicated by the bumps in the standard deviation curve.

Five regions were defined in each subarray (one in the center and four towards the corners) in order to investigate how the SRF varies across the FOV, which is expected to be smooth and gradual. Each region of ~5x5 bolometers was averaged in order to minimize noise artefacts from individual bolometers or bad scans. Interferograms exhibiting nonlinearity, flux jumping, or excess noise were filtered out. The total number of bolometers included in the average for each region after filtering is given in Table 4.

Table 4: The number of bolometers in each region of the 4 subarrays included in the average SRF calculation after bad scans have been filtered out.

Region	s4a	s4b	s8c	s8d
Total pixels	589	477	570	503
Upper Right	19	2	20	8
Lower Right	20	22	22	15
Upper Left	11	22	29	0
Lower Left	26	27	30	38
Centre	39	21	38	24

The SRF was determined by the same method for the three remaining FTS-2 sub-arrays at both 450 and 850 μm (s4a, s4b, s8d). The results for all 4 sub-arrays are summarized in Figure 9. There are minor differences in fringing and position of the band edges across the FOV which must be accounted for in the FTS-2 data reduction pipeline, but these differences are not considered to be a significant concern for SCUBA-2 photometric measurements. Furthermore, we cannot at present determine if these variations are intrinsic to the SCUBA-2 instrument or an artefact of the FTS optics.

Figure 10 compares the mean of the measured SRF for sub-arrays s8c and s8d to the response predicted by the linear product of the spectral transmissions of the individual components in the optical train shown in Figure 3. A shift between the theoretical and measured SRF is evident, likely due to the fact that the laboratory transmission measurements were performed at room temperature and the filter transmissions are expected to shift during cooling. This shift is expected to have a negligible effect on the performance of SCUBA-2. Figure 11 shows the same comparison for the 450 μm band, which does not exhibit the same frequency shift.

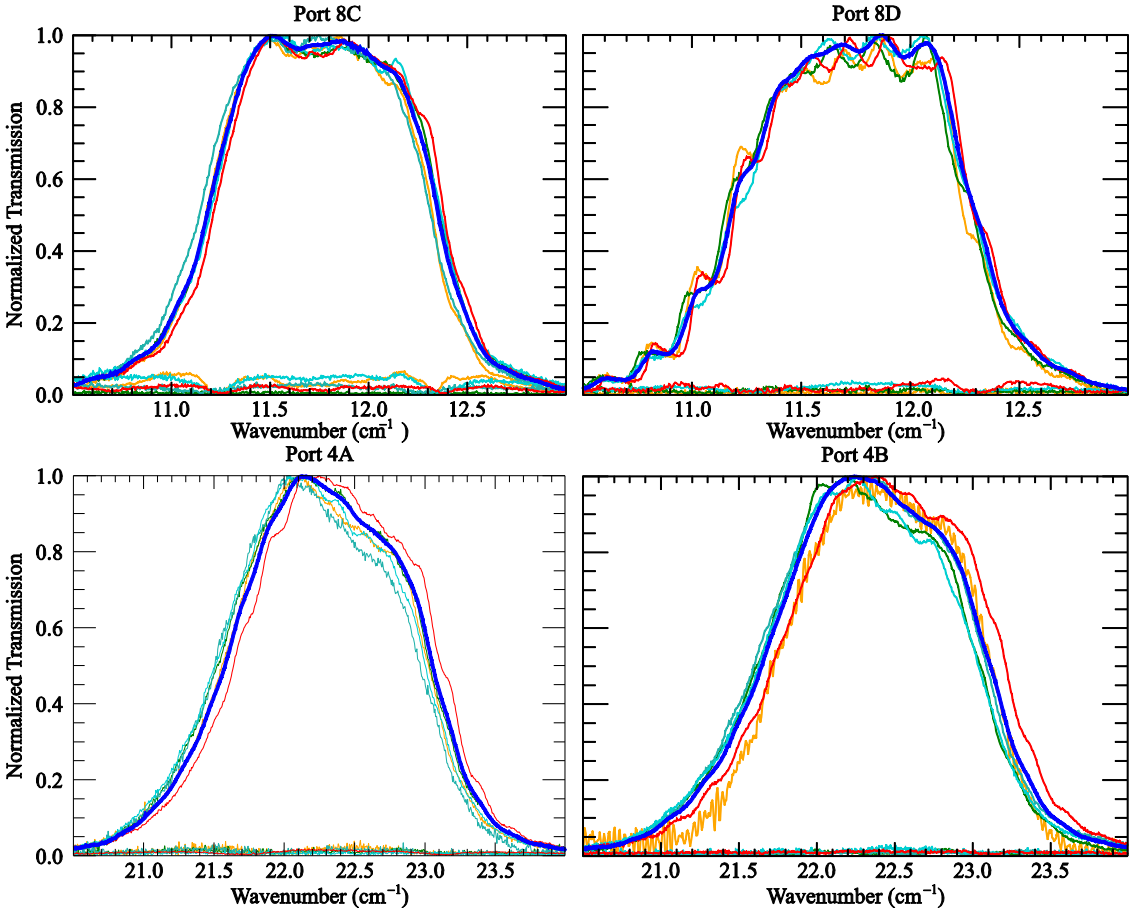

Figure 9: The average spectral response function for the four SCUBA-2 sub-arrays used by FTS-2 (thick blue line). Also shown are the SRF as determined from averages of the sub-regions of each sub-array (thin lines).

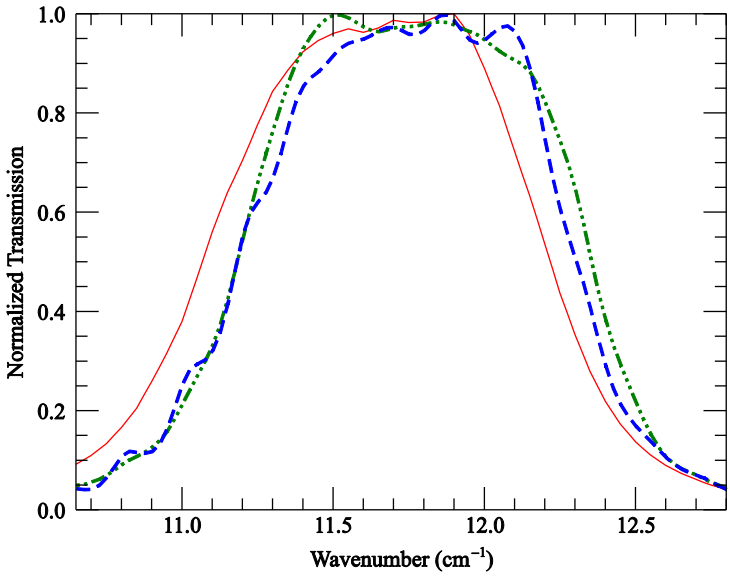

Figure 10. Comparison of theoretical SRF (solid red) calculated from room temperature measurements of individual filters and the SRF measured by FTS-2 (dash-dot green: s8c, dashed blue: s8d) for the 850 μm band.

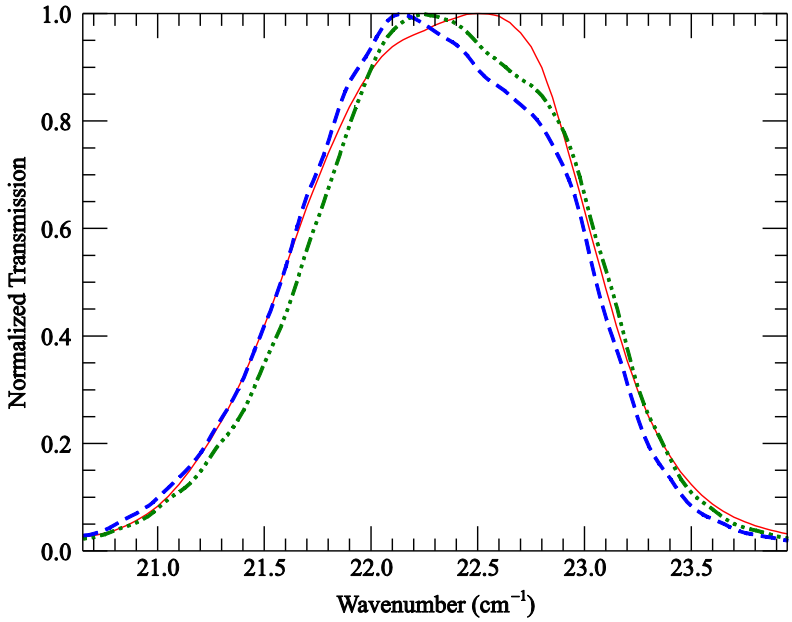

Figure 11. Comparison of theoretical SRF (solid red) calculated from room temperature measurements of individual filters and the SRF measured by FTS-2 (dashed blue: s4a, dash-dot green: s4b) for the 450 µm band.

4.2 Blackbody Temperature Retrieval

Since the blackbody measurements are in the Rayleigh-Jeans regime, and since the bolometer response is expected to be linear, the SRF determined by measurement of two blackbody temperatures can be used to determine the temperature of a third, unknown, blackbody temperature. If we assume that the reference port of the interferometer is at the same temperature for all measurements, the calculation can be simplified by computing Equation 7 instead of using the normalized SRF and the full Planck function:

$$SRF'(\sigma) = \frac{O_2(\sigma) - O_1(\sigma)}{\sigma^2 \cdot (T_2 - T_1)} \tag{7}$$

In this case, *SRF'* contains the scale factor including the optical efficiencies and throughput. The temperature of the unknown source can be determined directly as:

$$T_3(\sigma) = \frac{O_3(\sigma) - O_1(\sigma)}{SRF'(\sigma)} + T_1 \tag{8}$$

Figure 12 shows the retrieved temperature after applying Equations 7 and 8 to the measurement of a third blackbody temperature (25.3 °C). While the reference port temperatures were not identical in these three measurements (see Table 3), the correct temperature is obtained within the uncertainty of the thermometry. This is an indication that the bolometer response is linear, which is required for accurate SRF measurement. The temperature curve from Equation 8 is expected to be flat across the bandpass. If the SRF does not have the correct spectral curvature, the retrieved temperature curve will not be flat. As one might expect, using an SRF derived from an individual bolometer results in the best correction to that bolometer; using an average SRF derived from pixels across the array produces nonlinear results due to variation in spectral response across the array.

While the amplitude of the un-normalized SRF varies significantly across the array, variations in the band edges and fringing across the bandpass (which would not be corrected through normal photometric calibrations) are not large enough to cause significant errors in the SCUBA-2 photometric measurements.

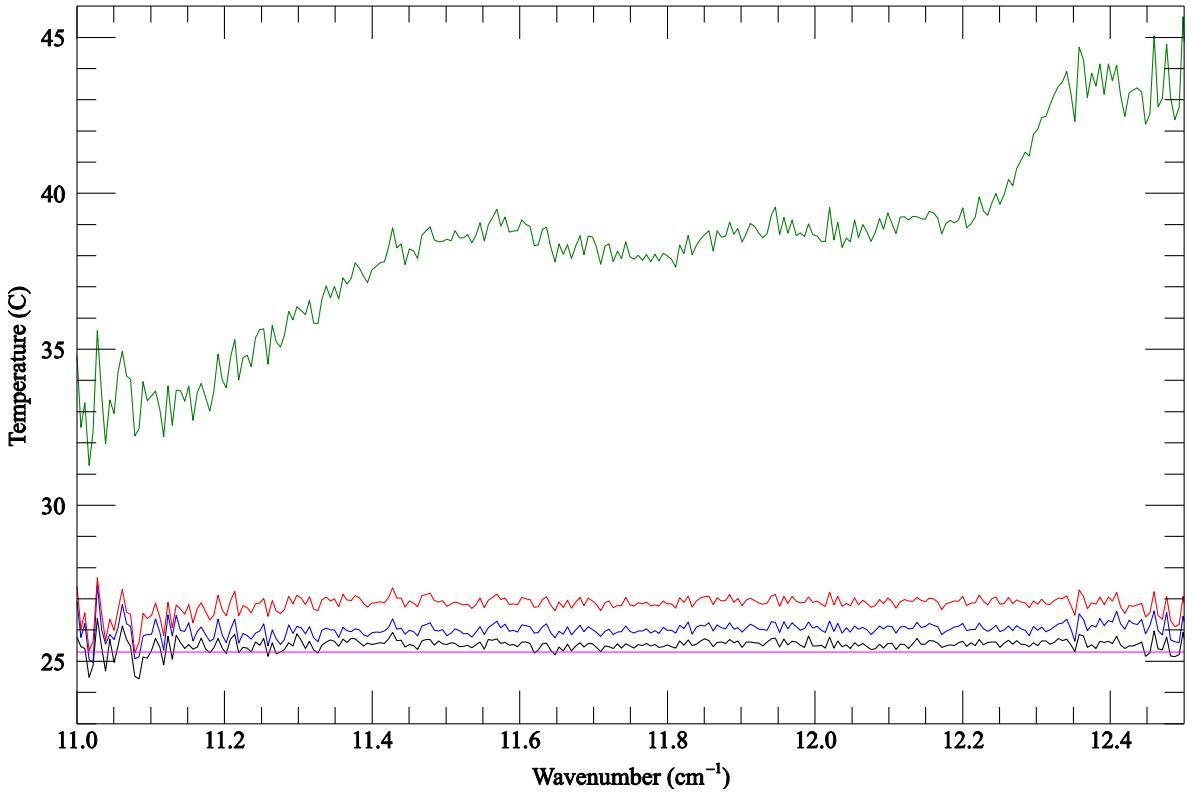

Figure 12. Retrieval of the blackbody temperature for bolometer (19,22) when using the SRF derived from the same bolometer (lower spectrum), the average of 2x2 neighboring bolometers (second lowest spectrum), the average of 3x3 neighboring bolometers (third lowest spectrum) and the average of all the active bolometers (top spectrum). The flat line shows the actual temperature measured on the blackbody heater (25.3 °C). Curvature in the retrieved temperature indicates poor characterization of the SRF.

5. CONCLUSIONS

In this paper we have described the technique for determining the spectral response function of the SCUBA-2 450 and 850 μm filter bands. Apart from a frequency shift due to temperature, the measured SRFs are in good agreement with those predicted from the linear combination of room temperature measurements of all components in the SCUBA-2 optical train. The derived SRFs have been validated on independent data and will find use in the interpretation of photometric images obtained with SCUBA-2.

6. AKNOWLEDGEMENTS

On behalf of the Canadian SCUBA-2 consortium, the authors acknowledge the support of a CFI international access award for Canadian participation in the SCUBA-2 project. David Naylor acknowledges support from NSERC and the CSA. The authors also acknowledge the assistance of the JAC staff during the FTS-2 measurements. The SCUBA-2 project is funded by the UK Particle Physics and Astronomy Research Council (PPARC), the JCMT Development Fund and the Canadian Foundation for Innovation (CFI).

REFERENCES

[1] W. S. Holland et al., “SCUBA-2: the 10,000 pixel bolometer camera on the James Clerk Maxwell Telescope,” Monthly Notices of the Royal Astronomical Society, 430, 2513 (2013).

[2] Bintley, D., “Cryostat Window, Filter and Dichroic Specification and Measurements,” Joint Astronomy Centre, 4 Jan 2012, http://www.jach.hawaii.edu/JCMT/continuum/scuba2/filter/.

[3] Leclerc, M.R., Gom, B.G., and Naylor, D.A., "Optical Design of the SCUBA-2 IFTS," Proc. SPIE, 701471 (2008).
[4] J. Buckle et al., "HARP/ACSIS: a submillimetre spectral imaging system on the James Clerk Maxwell Telescope," Monthly Notices of the Royal Astronomical Society, 399, 1026-1043 (2009).
[5] G. Pilbratt et al., "Herschel Space Observatory - An ESA facility for far-infrared and submillimetre astronomy," Astronomy and Astrophysics, 518, L1 (2010).
[6] M. J. Griffin et al., "The Herschel-SPIRE instrument and its in-flight performance," Astronomy and Astrophysics, 518, L3 (2010).
[7] Blue Sky Spectroscopy Inc., BTRAM Radiative Transfer Model, http://blueskyspectroscopy.com/products-and-services/btram-v3/
[8] Laird Technologies, Eccosorb AN72; http://www.eccosorb.com/products-eccosorb-an.htm
[9] Brad G. Gom et al., "SCUBA-2 Fourier transform spectrometer (FTS-2) commissioning results," Proc. SPIE, 915372 (2014).
[10] Naylor, D. A., Gom, B. G., Jones, S., Spencer, L., "Non-linear behaviour of bolometric detectors in Fourier spectroscopy," Optics and Photonics Congress Fourier Transform Spectroscopy Topical Meeting JTuB15, (2009).